LAWRENCE
LIVERMORE
NATIONAL
LABORATORY

LLNL-PROC-675458

Ignition and Growth Modeling of Detonation Reaction Zone Experiments on Single Crystals of PETN and HMX

B. W. White, C. M. Tarver

July 29, 2015

19th Biennial APS Conference on Shock Compression of Condensed Matter
Tampa, FL, United States
June 12, 2015 through June 17, 2015

Disclaimer

Ignition and Growth Modeling of Detonation Reaction Zone Experiments on Single Crystals of PETN and HMX

Bradley W. White[1] and Craig M. Tarver[1, a)]

[1]Lawrence Livermore National Laboratory, 7000 East Avenue, Livermore, CA 94551, USA

[a)]Corresponding author: tarver1@llnl.gov

Abstract. It has long been known that detonating single crystals of solid explosives have much larger failure diameters than those of heterogeneous charges of the same explosive pressed or cast to 98 – 99% theoretical maximum density (TMD). In 1957, Holland et al. demonstrated that PETN single crystals had failure diameters of about 8 mm, whereas heterogeneous PETN charges have failure diameters of less than 0.5 mm. Recently, Fedorov et al. quantitatively determined nanosecond time resolved detonation reaction zone profiles of single crystals of PETN and HMX by measuring the interface particle velocity histories of the detonating crystals and LiF windows using a PDV system. The measured reaction zone time durations for PETN and HMX single crystal detonations were approximately 100 and 260 nanoseconds, respectively. These experiments provided the necessary data to develop Ignition and Growth (I&G) reactive flow model parameters for the single crystal detonation reaction zones. Using these parameters, the calculated unconfined failure diameter of a PETN single crystal was 7.5 +/- 0.5 mm, close to the 8 mm experimental value. The calculated unconfined diameter of an unconfined HMX single crystal was 15 +/- 1 mm. The unconfined failure diameter of an HMX single crystal has not yet been determined precisely, but Fedorov et al. detonated 14 mm diameter crystals confined by detonating HMX-based plastic bonded explosives (PBX) without initially overdriving the HMX crystals.

Keywords: Single crystal detonation reaction zone, PETN, HMX, Ignition and Growth modeling
PACS: 82.33.Vx, 82.40.Fp

INTRODUCTION

Holland et al. [1] experimentally determined that PETN single crystals exhibit failure diameters of about 8 mm, whereas heterogeneous PETN charges pressed to 98 – 99% TMD have failure diameters less than 0.5 mm [2]. They also showed that PETN single crystals shock initiate like homogeneous liquid explosives, in which an observed time delay can be measured between the shock front arrival and a "thermal explosion" near the rear boundary of the explosive charge [3]. The "thermal explosion" then creates a "super" detonation that propagates through the shock compressed liquid at detonation velocities greater than the steady state Chapman-Jouguet (C-J) velocity. After the "super" detonation overtakes the original shock wave, its velocity decreases until the C-J velocity is reached. Pressed solid explosives initiate more rapidly at lower shock pressures as reacting "hot spots" are formed when the voids are collapsed by the initial shock. The reacting "hot spots" rapidly grow consuming the neighboring explosive particles and increasing the pressure and temperature as C-J detonation is approached [4]. No "super" detonation is observed in this case, unless the initial density is extremely close to TMD [5]. Recently, Fedorov et al. [6] reported nanosecond time resolved measurements of the interface particle velocity histories of detonating PETN and HMX single crystals with LiF windows. The measured reaction zone time durations for PETN and HMX single crystal detonations were approximately 100 and 260 nanoseconds, respectively. This experimental data provided the necessary information to develop equation of state and reaction rate parameters for PETN and HMX single crystal detonation reaction zones using the I&G reactive flow model [7]. These I&G model parameters were then used to calculate the unconfined failure diameters failure diameters of single crystal PETN and HMX, which were compared to the experimentally measured failure diameters.

FEDOROV ETAL. EXPERIMENTS

The experimental geometry of Fedorov et al. is shown in Fig.1. It consists of: (1) a plane wave generator; (2) a 40 mm long "primer" layer consisting of a 90% HMX / 10% binder plastic bonded explosive (PBX) to initiate HMX crystals or a 70% RDX / 30% TNT explosive to initiate PETN crystals; (3) a thin HMX PBX or 70% RDX / 30 % TNT layer to eliminate gaps; (4) the HMX or PETN single crystal (up to 36 mm long); (5) a confining cartridge of the HMX PBX or 70% RDX / 30 % TNT; (6) a ~1 μm thick aluminum coating on the LiF crystal for laser reflection; (7) the LiF crystal; and (8,9) the PDV system. Two interface particle velocity histories were measured at the detonating HMX or PETN crystal and LiF interface. The unreacted von Neumann spike, the fast reaction that produces the gaseous products, the slower formation of solid carbon products, and the product expansion behind the C-J state can be inferred from the records. The LiF window has a higher impedance than the explosive crystal, so the impact of the detonation wave sends a shock wave forward into the LiF and a reflected shock wave back into the reaction zone. The reflected shock raises the pressure and temperature in the reacting mixture, resulting in a faster reaction rate in the explosive adjacent to the window than in the rest of the explosive. The resulting reactive flow requires an accurate hydrodynamic model to interpret the effects of the various waves on the reaction rates.

THE IGNITION AND GROWTH REACTIVE FLOW MODEL

The Ignition and Growth reactive flow model uses two Jones-Wilkins-Lee (JWL) equations of state (EOS's), one for unreacted explosive and one for reaction products:

$$p = A\, e^{-R_1 V} + B\, e^{-R_2 V} + \omega \square C_v T \tag{1}$$

where p is pressure, V is relative volume, T is temperature, ω is the Gruneisen coefficient, C_v is the average heat capacity, and A, B, R_1 and R_2 are constants. These EOS's are fitted to unreacted Hugoniot and reaction product Hugoniot data. The three-term reaction rate equation is used:

$$dF/dt = \underset{0<F<F_{igmax}}{I(1-F)^b(\rho/\rho_0 - 1 - a)^x} + \underset{0<F<F_{G1max}}{G_1(1-F)^c F^d p^y} + \underset{F_{G2min}<F<1}{G_2(1-F)^e F^g p^z} \tag{2}$$

where F is the fraction reacted, t is time in μs, ρ is the current density in g/cm^3, ρ_o is the initial density, and p is pressure in Mbars. I, G_1, G_2, a, b, c, d, e, g, x, y, z, F_{igmax}, F_{G1max}.and F_{G2min} are constants. Pressure and temperature equilibration between the two phases are assumed. The unreacted JWL EOS's for PETN and HMX are fitted to the von Neumann spike states measured by Fedorov et al. The reaction product JWL EOS's are based on those for pressed HMX PBX's [8] and PETN explosives [5], using the experimental detonation velocities and calculated C-J pressures. Table 1 lists the I&G model parameters for a PETN single crystal, while Table 2 lists those for an HMX single crystal. C-J detonation models with reaction product JWL EOS's for the 90% HMX / 10% Viton HMX PBX (LX-10) or 70% RDX / 30% TNT were used to initiate the single crystals, and the LiF Gruneisen EOS (ρ_o = 2.638 g/cm3, c =5.15 km/s, S_1 = 1.35, S_2 = S_3 = a = 0, and γ□ = 0.34) is used in the calculations.

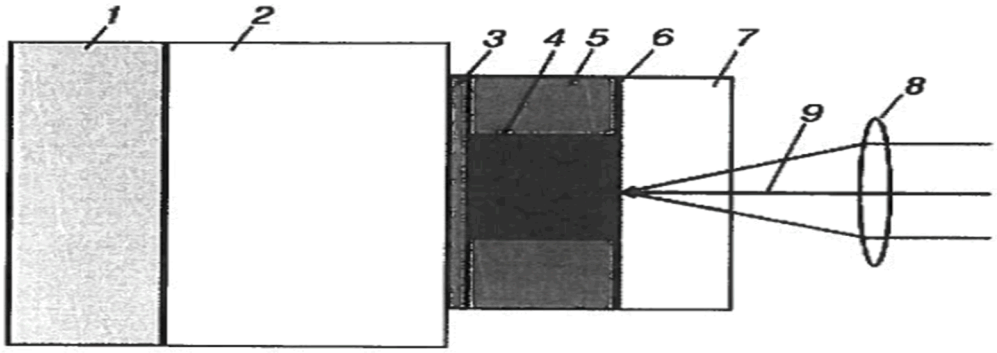

Figure 1. The arrangement of the Fedorov et al. experiment

COMPARISONS OF EXPERIMENTAL AND CALCULATIONAL RESULTS

The measured and calculated interface particle velocities for HMX single crystals are shown in Fig. 2, along with a calculation of an smaller scale experiment using pressed HMX based PBX 9501 (95% HMX / 2.5% Estane / 2.5% BDNPA/F) [9] and a calculation of Fedorov et al.'s experiment with the PBX 9501 I&G model [10] substituted for the HMX crystal. Fedorov et al. estimated the HMX crystal von Neumann spike pressure to be 60 GPa, so the unreacted HMX JWL EOS was set to yield a 60 GPa spike. Many 98 – 99% TMD HMX PBX detonation reaction zone profiles have been measured, and the observed von Neumann spike states are in the 42 – 45 GPa range [11,12]. So a 60 GPa von Neumann spike pressure for an HMX crystal seems high. The HMX I&G model assumes that 90% of the chemical energy is released in ~100 ns and that the last 10%, which is caused by slow solid carbon formation, requires another 120 ns. Fedorov et al. chose an interface particle velocity of 2.16 km/s at 265 ns as the sonic state. The calculated 100% reacted sonic state is 2.24 km/s at 220 ns. The magnitude, shape, and timing of the partially reacted states agree well. The two PBX 9501 calculations were added to Fig. 2 to show that PBX 9501 reacts completely in ~100 ns, has a lower von Neumann spike, and a lower C-J particle velocity than single crystal HMX. Fedorov et al. did not publish the interface particle velocity histories for detonating PETN. They did estimate von Neumann spike and C-J states based on the pressure – particle velocity curves shown in Fig. 3. They measured an initial interface particle velocity of 2.06 km/s, corresponding to a von Neumann spike pressure of 35.4 GPa and particle velocity of 2.42 km/s. They also chose a C-J pressure of 28 GPa and particle velocity of 1.88 km/s. Fedorov et al. inferred reaction times averaging 90 – 95 ns in seven experiments. Figure 4 shows the calculated PETN/LiF particle velocity histories for a PETN single crystal and a pressed PETN charge [5]. The initial interface

Table 1. Ignition and Growth model parameters for a PETN single crystal at 1.778 g/cm^3

Unreacted JWL EOS	Product JWL EOS	Reaction rate parameters
A = 7320 Mbar	A = 10.506 Mbar	I = 20000 μs^{-1} a = 0.0 x = 4.0 b = 0.667
B = -0.052654 Mbar	B = 0.93391 Mbar	F_{igmax} = 0.001 F_{G1max} = 0.9 F_{G2min} = 0.9
R_1 = 14.1	R_1 = 6.0	G_1 = 2810 $Mbar^{-3}\mu s^{-1}$ c = 0.667 d = 0.667
R_2 = 1.41	R_2 = 2.6	y = 3.0
ω = 0.8938	ω = 0.57	G_2 = 40 $Mbar^{-1}\mu s^{-1}$
Cv = 2.704e-5 Mbar/K	Cv = 1.0e-5 Mbar/K	z = 1.0
To = 298K	Eo = 0.10892 Mbar-cm^3/cm^3-g	e = 0.667 g = 0.667

Table 2. Ignition and Growth model parameters for an HMX single crystal at 1.905 g/cm^3

Unreacted JWL EOS	Product JWL EOS	Reaction rate parameters
A = 3000 Mbar	A = 14.0329Mbar	I = 20000 μs^{-1} a = 0.0 x = 4.0 b = 0.667
B = -0.039041 Mbar	B = 0.99913 Mbar	F_{igmax} = 0.001 F_{G1max} = 0.9 F_{G2min} = 0.9
R_1 = 14.1	R_1 = 5.9	G_1 = 200 $Mbar^{-3}\mu s^{-1}$ c = 0.667 d = 0.667
R_2 = 1.41	R_2 = 2.1	y = 3.0
ω = 0.8938	ω = 0.57	G_2 = 20 $Mbar^{-1}\mu s^{-1}$
Cv = 2.704e-5 Mbar/K	Cv = 1.0e-5 Mbar/K	z = 1.0
To = 298K	Eo = 0.10947 Mbar-cm^3/cm^3-g	e = 0.667 g = 0.667

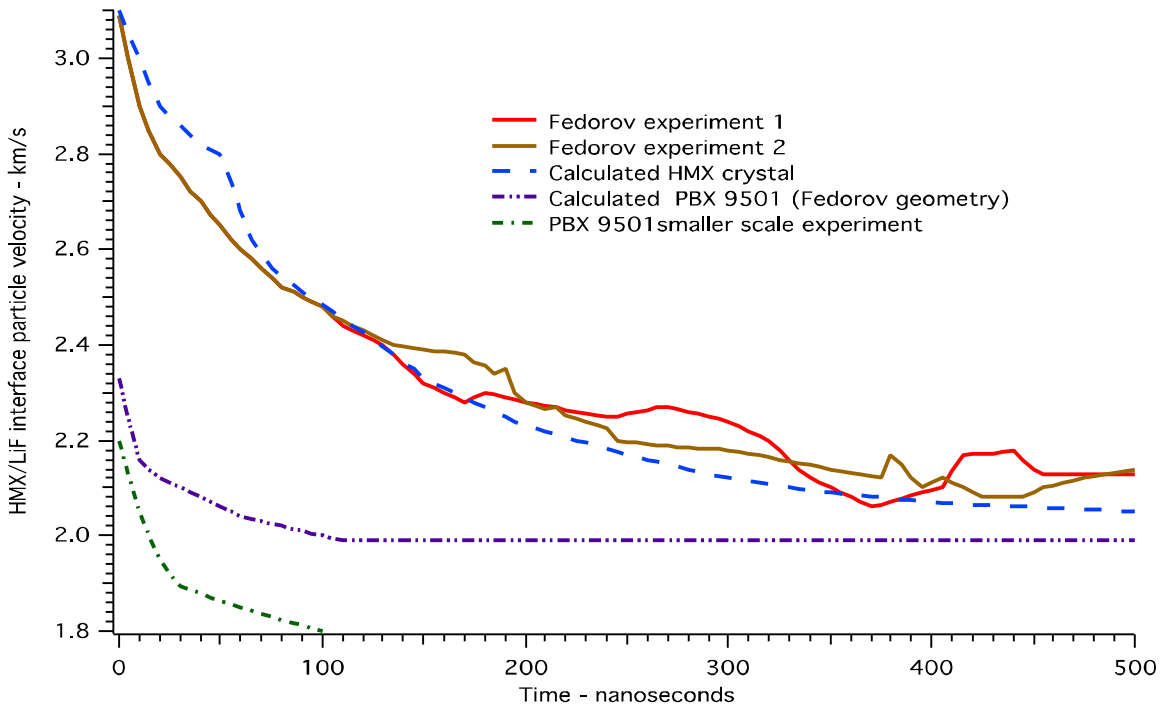

Figure 2. Measured and calculated HMX/LiF interface particle velocity histories for HMX and PBX 9501

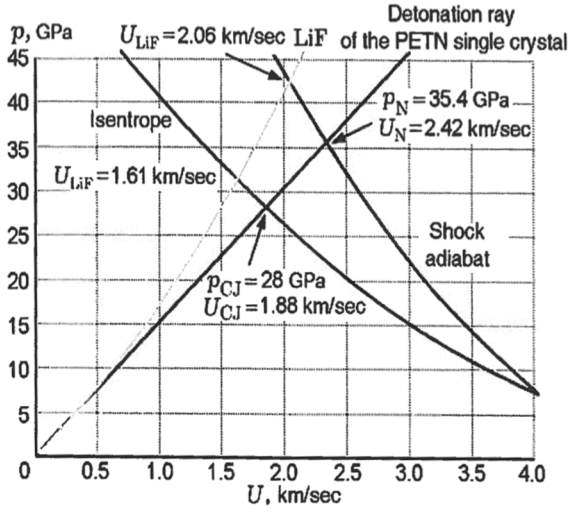

Figure 3. Federov pressure – particle velocity states

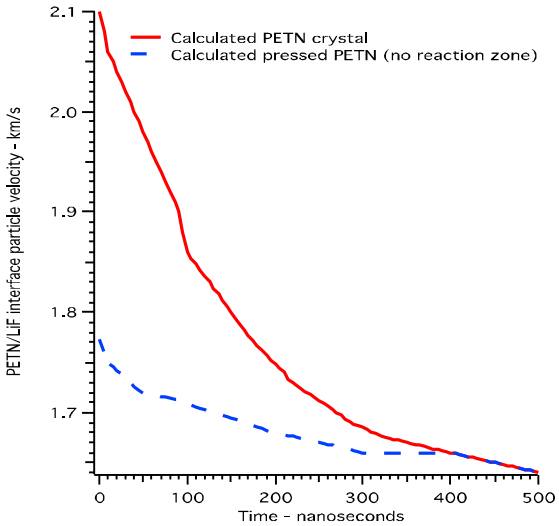

Figure 4. PETN interface particle velocities

velocity (2.09 km/s) agrees that of Fedorov et al., showing that the von Neumann spike states are similar. The calculated total reaction time is ~100 ns and corresponds to a C-J pressure of 32.1 GPa and an LiF interface velocity of 1.86 km/s. The 100 ns reaction time of pressed PETN charge is likely to be related to electrical conductivity measurements in detonating PETN [13,14] of 40 – 70 ns. Measured reaction zone times for pressed PETN are less than 5 to 10 ns [5,15,16]. The HMX and PETN I&G parameters are used to estimate unconfined failure diameters.

CALCULATED VERSUS EXPERIMENTAL FAILURE DIAMETERS

Holland et al. [1] determined the unconfined PETN single crystals to be approximately 8 mm. Using the PETN parameters in Table 1, the calculated unconfined cylindrical PETN failure diameter is 7.5 +/- 0.5 mm. The unconfined failure diameter of an HMX single crystal has never been measured exactly, but Fedorov et al. [6] detonated a 14 mm diameter crystal surrounded by and initiated by a 90% HMX / 10% binder PBX, which does not overdrive the HMX crystal. Using the HMX parameters in Table 2, the calculated unconfined cylindrical HMX failure diameter is 15 +/- 1 mm. The failure diameters of pressed PETN and HMX PBX's are less than 0.5 mm and 1 to 2 mm, respectively. The measured and calculated reaction zone lengths and failure diameters of HMX and PETN crystals are more than order of magnitude greater than those of pressed PETN and HMX explosives.

CONCLUSIONS

Fedorov et al.'s experiments on reaction zones of HMX and PETN single crystals provided the necessary data for I&G model development. The agreement between calculated unconfined failure diameters using these models and measured failure diameters is encouraging. Similar studies using other solid explosives would be very interesting.

ACKNOWLEDGEMENTS

This work was performed under the auspices of the U. S. Department of Energy by the Lawrence Livermore National Laboratory under Contract No. DE-AC52-07NA27344.

REFERENCES

1. T. E. Holland, A. W. Campbell, and M. E. Malin, J. Appl. Phys. **28**, 1217 (1957).
2. A. S. Tappan, R. Knepper, R, R. Wixom, J. C. Miller, M. P. Marquez, and J. P. Ball, "Critical Thickness Measurements in Vapor Deposited PETN Films," *Fourteenth International Detonation Symposium*, Office of Naval Research ONR-351-10-185, Coeur d'Alene, ID, April 11-16, 2010, pp. 1087-1095.
3. A. N. Dremin, *Toward Detonation Theory* (Springer-Verlag, New York, 1999), pp. 15-30.
4. E. L. Lee and C. M. Tarver, Phys. Fluids **23**, 2382 (1980).
5. C. M. Tarver, R. D. Breithaupt, and J. W. Kury, J. Appl. Phys. **81**, 7193-7202 (1997).
6. A. V. Fedorov, A. L. Mikhailov, L. K. Antonyuk, D. V. Nazorov, and S. A. Finyushin, Combustion Explosion, and Shock Waves **47**, 601-605 (2011).
7. C. M. Tarver, J. O. Hallquist, and L. M. Erickson, "Modeling Short Pulse Duration Shock Initiation of Solid Explosives," *Eighth Symposium (International) on Detonation*, Naval Surface Weapons Center NSWC MP-86-194, Albuquerque, NM, July 15-19, 1985, pp. 951-961.
8. K. S. Vandersall, C. M. Tarver, F. Garcia, and S. K. Chidester, J. Appl. Phys. **107**, 094906 (2010).
9. R. L. Gustavsen, S. A. Sheffield, and R. R. Alcon, "Detonation Wave Profiles in HMX Based Explosives," in *Shock Compression of Condensed Matter-1997*, AIP Conf. Proc. 429, S. C. Schmidt, ed., Amherst, MA, July 27 – August 1, 1997, pp. 739-742.
10. C. M. Tarver, "Ignition and Growth Reactive Flow Modeling of Recent HMX/TATB Experiments," paper submitted for publication in these Proceedings.
11. B. Hayes and C. M. Tarver, "Interpolation of Detonation Parameters from Experimental Particle Velocity Records," *Seventh Symposium (International) on Detonation*, Naval Surface Weapons Center NSWC MP-82-334, Annapolis, MD, June 16-19, 1981, pp. 1029-1039.
12. S. A. Sheffield, D. D. Bloomquist, and C. M. Tarver, J. Chem. Phys. **80**, 3831-3844 (1984).
13. B, Hayes, "On the Electrical Conductivity in Detonation Products," *Fourth Symposium (International) on Detonation*, Office of Naval Research ACR-126, White Oak, MD, October 12-15, 1965, pp. 595-601.
14. A. P. Ershov, N. P. Satonkina, and G. M. Inanov, "Reaction Zones and Conductive Zones in Dense Explosives," *Thirteenth International Detonation Symposium*, Office of Naval Research ONR-351-07-01, Norfolk, VA, pp. 79-88.
15. B. G. Loboiko and S. N. Lubyatinsky, *Combustion, Explosion, and Shock Waves* **36**, 716-733 (2000).
16. A. V. Fedorov, *Khim. Fiz.* **24(10)**, 13-22 (2005).